

1 **Integrated Environment-Occupant-Pathogen Information Modeling to Assess and**
2 **Communicate Room-Level Outbreak Risks of Infectious Diseases**

3

4 **Abstract**

5 Microbial pathogen transmission within built environments is a main public health concern. The
6 pandemic of coronavirus disease 2019 (COVID-19) adds to the urgency of developing effective
7 means to reduce the pathogen transmission in mass-gathering public buildings such as schools,
8 hospitals, and airports. To inform occupants and guide facility managers to prevent and respond
9 to infectious disease outbreaks, this study proposed a framework to assess the room-level
10 outbreak risks in buildings by modeling built environment characteristics, occupancy
11 information, and pathogen transmission. Building information modeling (BIM) is exploited to
12 automatically retrieve building parameters and possible occupant interactions that are relevant
13 to pathogen transmission. The extracted information is fed into an environment pathogen
14 transmission model to derive the basic reproduction numbers for different pathogens, which
15 serve as proxies of outbreak potentials in rooms. A web-based system is developed to provide
16 timely information regarding outbreak risks to occupants and facility managers. The efficacy of
17 the proposed method was demonstrated by a case study, in which the building characteristics,
18 occupancy schedules, pathogen parameters, as well as hygiene and cleaning practices are
19 considered for outbreak risk assessment. This study contributes to the body of knowledge by
20 computationally integrating building, occupant, and pathogen information modeling for infectious
21 disease outbreak assessment, and communicating actionable information for built environment
22 management.

23

24 **Keywords**

25 Building Information Modeling; Pathogen Transmission; Outbreak Risk; COVID-19; Health

26

27 **1. Introduction**

28 People spend most of their time in buildings, including homes, offices, schools, stores,
29 restaurants, theaters, and many others. The buildings become hotspots for pathogen
30 transmission and exposure, decimating populations through epidemics and everyday infections.
31 The disastrous impacts of infectious diseases highlight the urgent need to reduce the
32 transmission of pathogens, and their exposure to occupants in buildings. Humans can be
33 infected by microbial pathogens via contacting contaminated objects, referred to as fomites.
34 Fomite-based transmission is an important route in built environments for transferring disease-
35 causing microbiomes to a new human host [1]. The mechanism of fomite-mediated transmission
36 involves three steps. First, a surface is contaminated by infectious pathogens. The
37 contamination can occur when an infected person touches the surface or bioaerosols containing
38 pathogens settle down on the surface. Second, a person touches a contaminated surface with
39 his or her hand, transferring the pathogens to the hand. Third, the person touches susceptible
40 sites (mucous membranes) on his or her body with the contaminated hand, which inoculates the
41 site with pathogens, resulting in potential infection. A recent study [2] found that contamination
42 of a single doorknob or tabletop can spread the infectious pathogens to other commonly
43 touched objects, exposing 40-60% of people in the buildings.

44

45 Many pathogens can be transmitted via fomites. For example, during flu seasons, measurable
46 levels of influenza virus can be found on all common building surfaces [1,3], underlining the
47 importance of fomite in influenza transmission. The pandemic of coronavirus disease 2019
48 (COVID-19) has swept the entire world with more than 29.6 million infections and 935,898
49 deaths as of September 16, 2020 [4]. During the pandemic of COVID-19, viable severe acute
50 respiratory syndrome coronavirus 2 (SARS-CoV-2) can be detected on various surfaces. High

51 concentration of SARS-CoV-2 are found on surfaces in healthcare facilities where COVID-19
52 patients are treated [5,6]. Norovirus can also be transmitted via fomite [7,8], causing 93% of
53 nonbacterial gastroenteritis outbreaks in the U.S. In addition, pathogens including
54 *staphylococcus aureus*, *Clostridium difficile*, *Staphylococcus aureus*, *Pseudomonas aeruginosa*,
55 *Pseudomonas putida*, and *Enterococcus faecalis* can also be transmitted by surface contact [9].
56

57 Models have been developed for environmental risk assessment and environmental infection
58 transmission [10]. Fomite-mediated transmission has received increased attention [11,12]. To
59 assess pathogen transmission to susceptible hosts, the models such as the environmental
60 infection transmission system modeling framework consider the dynamics of contact and
61 pathogen transfer between individuals via their hands and fomites, pathogen persistence in the
62 environment, pathogen shedding, and recovery of infected individuals. Studies [13–15] also
63 exploited experimentation approaches to measure the transfer of microbiomes between fomites
64 and humans. The measured microbiological and epidemiological data can be used to assess
65 the transmissibility of the pathogens and used in the models for risk assessment. Despite
66 research efforts made in epidemiology, the modeling of building, occupant, and pathogen has
67 not been well linked to predict the microbial burdens and outbreak risks.
68

69 Predicting outbreak risks in buildings and communicating actionable information to occupants
70 and facility managers are challenging. First, pathogen burdens could differ considerably in
71 rooms even in the same building. Building design and operation can influence indoor microbial
72 communities [16,17]. The microbial communities in different rooms with different functionalities
73 and spatial configurations are found to exhibit very different patterns [18,19]. Occupancy also
74 significantly affects the microbial communities in buildings. For example, bacteria taxa in spaces
75 with a high occupant diversity and a high degree of physical connectedness are different from
76 that in spaces with low levels of connectedness and occupant diversity [16]. Humans can
77 transfer microbiomes including pathogens to the environment via skin-to-surface contact and
78 direct shedding of large biological particles [20,21]. The microbial exchange between occupants
79 and surfaces can occur in both directions [12]. With different uses and occupancy levels,
80 outbreak risks could vary depending on the locations in a building, underlining the need for a
81 spatially-adapted modeling approach. However, there lacks a computational modeling approach
82 to link the coupled physical-biological processes of buildings, occupants, and pathogens to
83 automatically assess the spatially-varying infection and outbreak risks at unprecedented scales.
84 Therefore, it is imperative to establish the computational framework to quickly compute the risk
85 in buildings to inform end-users and guide adaptive operations.
86

87 Second, due to the absence of an effective means for information communication, end-users
88 have limited access to easy-to-understand information regarding the outbreak risks to make
89 necessary interventions. Building information modeling (BIM) uses standardized machine-
90 readable information created or gathered about a facility throughout its lifecycle for all
91 stakeholders involved [22]. Information can be extracted from building information models, as
92 they are the shared digital representations of physical and functional characteristics of any built
93 objects [22]. In addition, BIM has also been used as a powerful tool to visualize the parametric
94 building model with computed rich information [23]. However, to the authors' best knowledge,
95 existing studies have not explored the capability of BIM in environmental pathogenic infection
96 assessment, and leverage BIM as a platform to visualize and communicate outbreak risk
97 information to end-users for facility management.
98

99 This study aims to develop a framework for room-level outbreak risk assessment based on
100 integrated building-occupancy-pathogen modeling to mitigate the spread of infectious disease in
101 buildings. The rationale is twofold. First, buildings are highly heterogeneous with a variety of

102 compartments of distinctive functionalities and characteristics, providing diverse habitats for
 103 humans and various pathogens [17,18]. Modeling the pathogen transmission and exposure
 104 within a building at the room level will provide useful information at an unprecedented resolution
 105 to implement appropriate disease control strategies. Second, the spread of infectious diseases
 106 can be mitigated if occupants and facility managers have adequate and timely information
 107 regarding the outbreak risks within their buildings. Communicating actionable information to
 108 occupants and facility managers through an easily accessible interface will help occupants to
 109 follow hygiene and social distancing practice, and help facility managers to schedule disinfection
 110 for rooms with high outbreak risks.

111

112 **2. Method**

113 To address the knowledge gaps, a novel environment-occupant-pathogen modeling framework
 114 and a web-based information visualization system are developed to assess the outbreak risks
 115 and mitigate the spread of infectious diseases in buildings (Fig. 1). First, to assess the outbreak
 116 risks, the fomite-based pathogen transmission model proposed in [24] is adopted in this study.
 117 The limitation of the model is that the environmental parameters and occupant characteristics
 118 are not automatically extracted and incorporated in the model, hindering the computation of the
 119 spatially-varying environmental infection risks in buildings. To overcome this limitation, BIM is
 120 exploited to automatically retrieve venue-specific parameters including building characteristics
 121 and occupancy information that are relevant to pathogen transmission and exposure. Then, the
 122 extracted building and occupant parameters are used with pathogen-specific parameters in a
 123 human-building-pathogen transmission model to compute the basic reproduction number R_0 for
 124 each room in a building. R_0 is used as a proxy to assess the outbreak risks of different infectious
 125 diseases. Second, a web-based system is developed to enable information visualization and
 126 communication in an interactive manner to provide guidance for occupants and facility
 127 managers. This study innovatively establishes the computational links among building,
 128 occupant, and pathogen modeling to predict outbreak risks. The risk prediction for spatially and
 129 functionally distributed rooms in a building provides useful information for end-users to combat
 130 and respond to the spread of infectious diseases, including the seasonal flu and COVID-19. The
 131 developed method and system add a health dimension to transform the current building
 132 management to a user-centric and bio-informed paradigm.

133

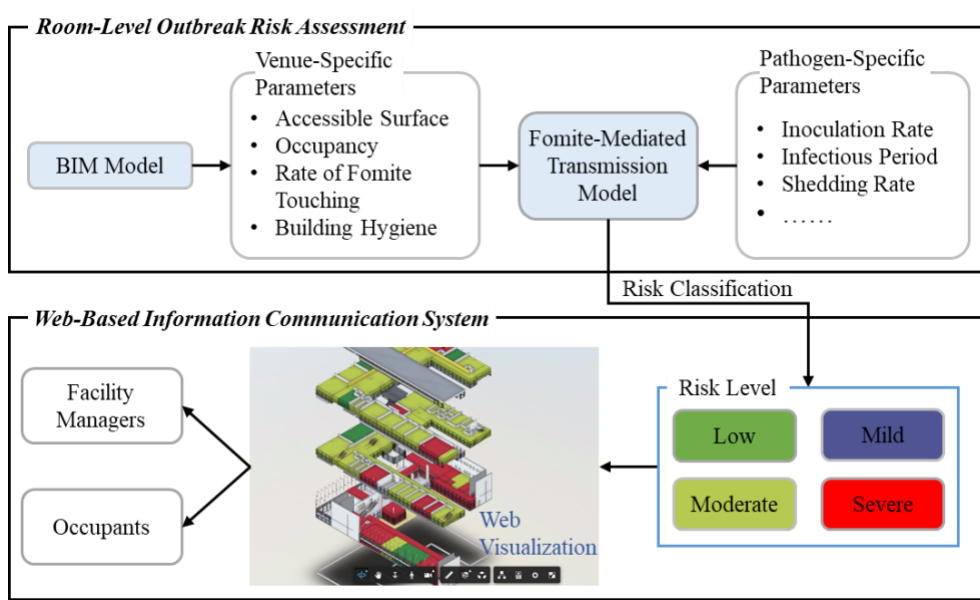
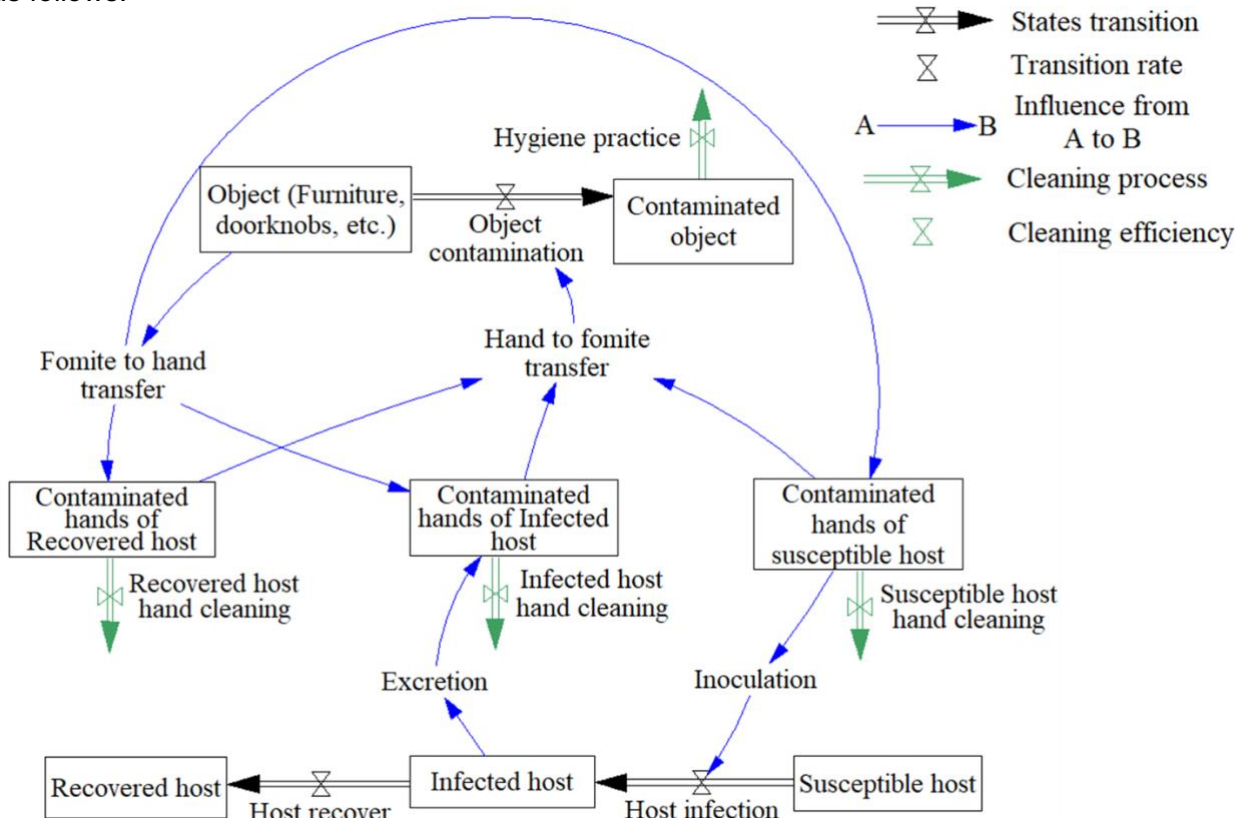


Fig. 1. Research Framework

134
 135

136 **2.1. Room-Level Outbreak Risk Assessment**

137 Employing the model proposed in [24], individuals are divided into three categories, i.e.,
 138 susceptible, infectious, and recovered. Pathogens may survive outside the host and
 139 contaminate either object surfaces or human hands. The pathogen exchange in built
 140 environments can occur through hand-surface contacts. Contaminated hands of hosts can
 141 contaminate surfaces of accessible objects, while susceptible people can get infected by
 142 touching the contaminated surfaces and self-inoculation. Fig. 2 shows the fomite-mediated
 143 pathogen transmission process in built environments. Building characteristics, occupant
 144 behavior, and pathogen parameters collectively determine the transmission ability through the
 145 dynamic processes of pathogen inoculation, fomite touching and transfer, pathogen excretion,
 146 pathogen decay, individual recovery, and building disinfection and individual hygiene.
 147 Characteristics of the built environment (e.g., contaminated objects and building hygiene) and
 148 occupant behavior (e.g., fomite touching and hand cleaning) are critical in the process of fomite-
 149 mediated pathogen transmission in the built environment and are considered as venue-specific
 150 parameters. In addition, the transmission efficiency of different diseases also depends on
 151 pathogen-specific parameters, such as recovery rates and pathogen excretion. The
 152 determination and acquisition of venue-specific and pathogen-specific parameters are detailed
 153 as follows.



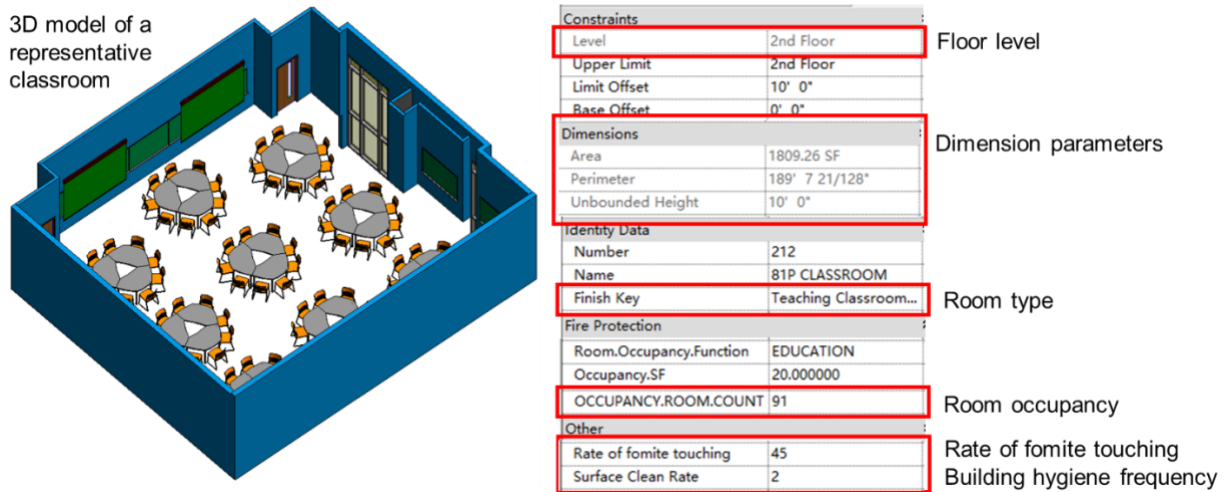
154
 155 **Fig. 2. Fomite-mediated pathogen transmission in built environments (Adapted from [24])**

156
 157 **2.1.1. Venue-specific parameters**

158 Because venue-specific parameters vary across rooms with different functions and occupancy
 159 levels, it is important to develop an effective means to accurately and automatically extract the
 160 venue-specific parameters to assess the outbreak risks at the resolution of room level. A
 161 building information model captures the relationships among different elements in a building,
 162 and allows the storage and extraction of detailed geometric and non-geometric information in a

163 3D virtual representation. The non-geometric information includes semantic and topological
 164 information, describing the attributes of elements and the relationship between components,
 165 respectively [25]. Hence, it is feasible and efficient to extract venue-specific parameters from a
 166 building information model.

167
 168 The BIM model can be divided into six Levels of Development (LOD) [26] that are suitable for
 169 conceptual design (LOD 100), schematic design (LOD 200), design development (LOD 300),
 170 construction documentation (LOD 350), fabrication and assembly (LOD 400), and maintenance
 171 and operation (LOD 500). To effectively capture the characteristics of buildings and occupants,
 172 this study uses LOD 500 BIM model that reflects the as-built conditions regarding the geometry
 173 information and non-graphical building attributes, as well as occupancy information. Fig. 3
 174 shows an example of a representative classroom in the BIM model. For most public buildings
 175 such as schools and hospitals, and particularly during the pandemic, the occupancy can be
 176 predetermined and incorporated in the BIM model as attributes.



178
 179 **Fig. 3. Building and Occupancy Information Modeling**

180
 181 The following venue-specific parameters will be extracted from the model.

182
 183 1) **Accessible surface.** The surfaces of objects, including doorknobs, stair railings, tables, and
 184 chairs, which people frequently interact with are considered as accessible surfaces. The
 185 accessible surface is computed as the summation of surface area of all touchable objects in
 186 a room. The proportion of accessible surface λ is defined as the ratio of accessible surface
 187 to the total area of surfaces within a room that includes both accessible surface and interior
 188 surface. The calculation is shown in Eq. 1.

$$\lambda = \frac{\sum \text{Accessible surface area}}{\sum \text{Accessible surface area} + \text{Room}_{\text{InnerArea}}} \quad (1)$$

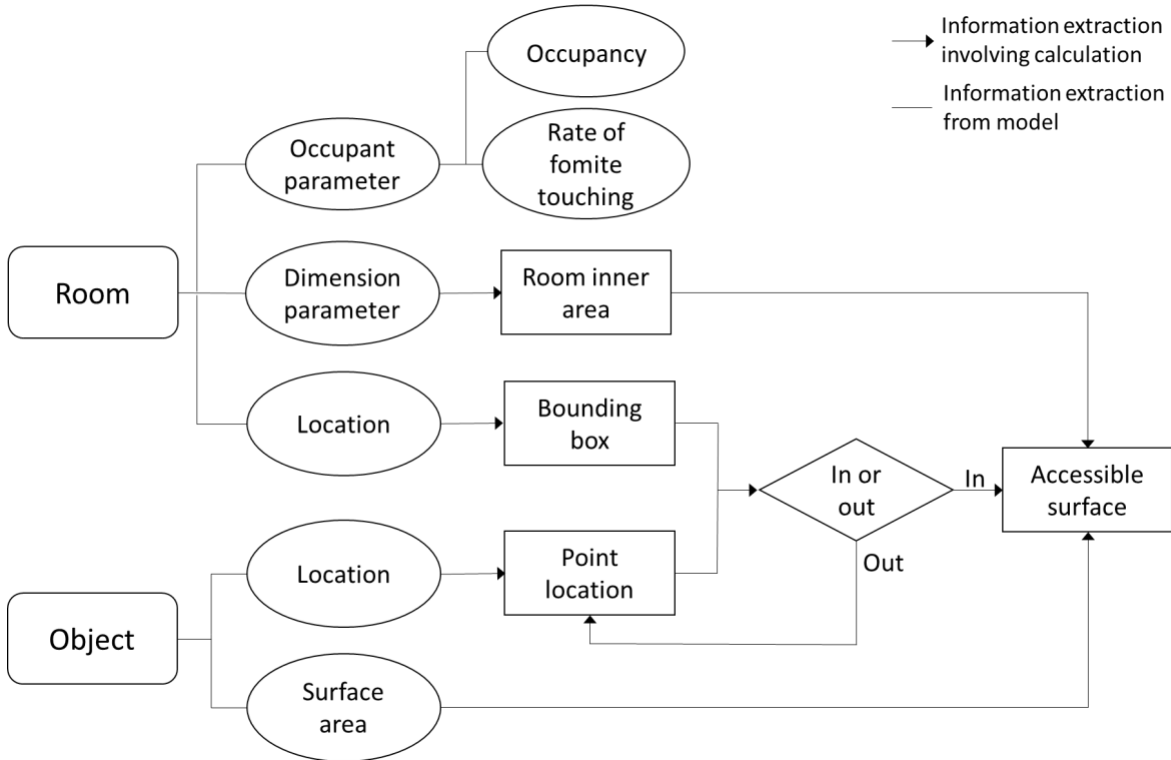
189
 190 2) **Occupancy.** The occupancy is the number of individuals present in a room per day. In this
 191 study, it is assumed that the occupancy of each room is predefined based on room capacity.
 192 During the pandemic of COVID-19, many buildings such as university campus buildings and
 193 office buildings have developed detailed occupancy schedules, which can be updated in the
 194 BIM model and then extracted for analysis. Consistent with the prior study [24], it is
 195 assumed that all individuals are identical within each room regarding susceptibility, contact
 196 rates, and infectiousness as well as other individual characteristics. This assumption

198 simplifies the model to capture the complex nature of pathogen transmission process. The
199 only difference among the individuals is the state associated with them: Susceptible S ,
200 Infected I , or Recovered R during the pathogen transmission process.
201

202 3) *Rate of fomite touching.* The rate of fomite touching is the frequency that occupants interact
203 with the objects inside a room on an hourly basis. A higher frequency of interaction indicates
204 a higher possibility of pathogen transmission between objects and hosts. In this study, the
205 rate of fomite touching is determined based on different functionalities of the rooms
206 considering the primary age group present in the rooms. For example, classrooms and
207 offices in a school building are two main types of rooms considered in this study. It is
208 assumed that the rate of fomite touching in classrooms is higher than that in offices because
209 the occupants in classrooms are younger people who are more likely to interact with the
210 built environment. According to the observations in [27], an average rate of touching
211 common areas (e.g., chairs, desks, facilities) in a school office is 12 times per hour.
212 Therefore, in this study, the rate of fomite touching is set as 12 times per hour for offices,
213 and that for classrooms is set as 45 times per hour based on [28]. Furthermore, to
214 incorporate the possible variation in different scenarios, a range of (0, 30) and (30, 60) is
215 considered for offices and classrooms, which also aligns with the setting in [28]. Analyses
216 will be conducted to examine the influence of the rate of fomite touching on outbreak risk.
217

218 4) *Building Cleaning and Hand Hygiene.* Building cleaning plays an important role in object
219 decontamination. For fomite-mediated transmission, surface cleaning can significantly
220 decrease the pathogen reproductive process. The frequency of building cleaning is
221 determined by the adopted sanitation schedule of the building. Hand hygiene removes
222 pathogens picked up from contaminated objects. For infected individuals, hand cleaning
223 also removes pathogens excreted to hand, and thus, preventing contaminating objects
224 through hand touching.
225

226 In this study, a computational tool is developed based on Dynamo [29] to extract the geometry
227 and properties of each room in a building, and to compute the corresponding venue-specific
228 parameters. Fig. 4 shows the workflow of the information retrieval process. Lines in Fig. 4
229 indicate direct information retrieval from the models and arrows indicate the information retrieval
230 involving calculations.
231



232
 233
 234
 235 The workflow for information retrieval is detailed as follows.
 236
 237 The steps for *extracting room parameters* are:
 238 1) Room element selection. Starting from a building information model, all elements are
 239 selected from the Room category, which is a predefined category including all the rooms in
 240 the model.
 241 2) Room information extraction. The essential room-related and occupant-related parameters
 242 are extracted from all the room elements. The room-related parameters include room area
 243 (the floor area of each room, named $room_A$), room perimeter (the summation of the length of
 244 all walls, named $room_P$), room height (the height of the walls, named $room_H$) and the rate of
 245 building hygiene. Occupant-related parameters include room occupancy and rate of fomite
 246 touching. With room dimension parameters, the interior surface of a room ($room_{InnerArea}$)
 247 can be calculated by Eq. 2:
 248
 249
$$room_{InnerArea} = 2 * room_A + room_P * room_H \quad (2)$$

 250
 251 3) Acquisition of room bounding box. The bounding box of a room element indicates the
 252 location of the boundaries of the room and is defined by two 3D point coordinates, i.e., the
 253 minimum point and maximum point. The bounding box can be used to determine if an object
 254 is inside a room by checking if the coordinate of an object is inside the range from the
 255 minimum point to the maximum point. The bounding box results are used for object
 256 parameter extraction.
 257
 258 Objects in the rooms such as furniture can be contaminated via hand-surface contact, and
 259 involved in the fomite transmission pathway. The furniture in a room is considered as accessible
 260 object.

261
262 The steps for extracting the object parameters are:
263 1) Furniture element selection. All the elements under the category “Furniture” are selected
264 from the model. This category contains information of all the furniture in the model.
265
266 2) Furniture information extraction. The essential furniture parameters are extracted from all
267 the furniture elements. The parameters include area (the surface area of furniture) and
268 location (the point location of each furniture element). The location of furniture is
269 transformed to a 3D point (a point with x, y, z coordinates) using a default function in
270 Dynamo. The coordinates represent the location of the furniture.
271
272 3) Location relationship between room and furniture. For each room element, the coordinates
273 of furniture in the model are compared with the coordinates of the room bounding box. This
274 process checks the 3D location relationship between each room and furniture.
275

276 Thereafter, the total furniture area in each room (Named $furniture_A$) is calculated by summing
277 up the surface area of all furniture inside the room. The proportion of accessible surface (λ) of
278 each room is calculated using Eq. 3.
279

$$\lambda = \frac{furniture_A}{furniture_A + room_{innerArea}} \quad (3)$$

280
281 **2.1.2. Pathogen-specific parameters**

282 Pathogen characteristics affect the transmission process through inoculation, excretion,
283 inactivation (decay), and recovery. According to the study [24], Table 1 lists the pathogen-
284 specific parameters used in the fomite-mediated transmission model.
285

286 **Table 1.** Description of pathogen parameters

Pathogen parameters	Symbol	Unit	Parameter description
Infectious period	$1/\gamma$	days	The period that an infectious individual can excrete and transmit pathogens
Shedding rate	α	pathogens/ (hours × people)	Infectious individual releases pathogens at rate α
Pathogen inactivation rate on surfaces	μ_F	1/hours	Pathogens decay at rate μ_F on surfaces
Pathogen inactivation rate on hands	μ_H	1/hours	Pathogens decay at rate μ_H on hands
Transfer efficiency from fomite to hand	τ_{FH}	1/touch	Pathogens transfer from fomite to hand at rate τ_{FH}
Transfer efficiency from hand to fomite	τ_{HF}	1/touch	Pathogens transfer from hand to fomite at rate τ_{HF}
Pathogen excreted to hand	φ_H	unitless	The proportion that pathogens are shed on hands
Dose response of pathogens on mucosa	π	unitless	The infectivity of a pathogen
Inoculation rate	ρ	1/hours	Rate of touching mouth or other routes of infection

288 In this study, three pathogens, i.e., influenza, norovirus, and SARS-CoV-2 are considered.
 289 Table 2 shows the parameter values used in the model. The pathogen-specific parameters of
 290 the first two viruses are determined based on [24]. The parameters of SARS-CoV-2 were
 291 determined based on a number of studies up to date. For the parameters that are still under
 292 research, the values are set based on surrogate viruses and assumptions, which are described
 293 as follows.
 294

295 **Table 2.** Values of pathogen-specific parameters of four viruses

Pathogen-specific parameter	Influenza	Norovirus	SARS-CoV-2
$1/\gamma$	6	15	8 [30] 1.99E4 (1.8E3, 2.39E4)
α	1E4	2.88E3	
μ_F	0.121	0.288	0.059
μ_H	88.2	1.07	0.8
τ_{FH}	0.1	0.07	0.37
τ_{HF}	0.025	0.13	0.14
φ_H	0.15	0.9	0.15
π	6.93E-05	4.78E-04	6.58E-06 [31]
ρ	15.8	15.8	15.8

296

297 1) The inactivation rates on surfaces (μ_F) and hands (μ_H). The inactivation rate on surfaces is
 298 determined based on the study [32], which provides the half-life of infectivity ($t_{0.5}$) on
 299 surfaces under common temperature and relative humidity. The inactivation process of the
 300 virus is assumed as a first-order kinetic model in this paper, and the inactivation rate is
 301 calculated as $\ln 2/t_{0.5}$. Under the circumstance of 74°F and 40 of relative humidity, the
 302 estimated half-life of infectivity on surfaces is 11.78 hours, and the approximate inactivation
 303 rate is 0.059 per hour. Due to the lack of exact data of μ_H , the parameter inactivation rate on
 304 skin of Middle East Respiratory Syndrome (MERS-CoV) is used in the paper, which is 0.8
 305 per hour [33].
 306

307 2) Transfer efficiency from fomite to hand (τ_{FH}) and transfer efficiency from hand to fomite
 308 (τ_{HF}). The transfer efficiency coefficients are estimated using parameters of MERS-CoV in
 309 [33] due to the absence of data. The transfer efficiency varies with surface materials.
 310 Compared with porous surfaces (e.g. fabrics, clothes, and sponges), non-porous surfaces
 311 such as desks, chairs, and door handles are more appropriate to represent the material of
 312 furniture surfaces considered in this paper. Thus, the transfer rates between hands and non-
 313 porous surfaces are used to indicate the transfer efficiency between hands and fomites.
 314 According to the results in [33], τ_{FH} is set as 0.37, and τ_{HF} is set as 0.14.
 315

316 3) Pathogen excreted to hand (φ_H). Because the virus excretion behavior of SARS-CoV-2 such
 317 as coughing, sneezing, and exhaling is similar to the excretion behavior of influenza, φ_H of
 318 SARS-CoV-2 is estimated using the same parameter of influenza.
 319

320 4) Shedding rate (α). In the paper, coughing is considered as the primary way for virus
 321 shedding. The shedding rate is determined by the number of viruses in the respiratory tract
 322 that is shed via coughing per hour per infectious individual. The equation for shedding rate
 323 calculation is shown in Eq. 4.

$$\alpha = V_{droplet} \times F_{cough} \times N_{droplet} \times L \quad (4)$$

324 $V_{droplet}$ indicates the volume per infectious droplet in cm^3 , F_{cough} is the coughing frequency
 325 per hour, $N_{droplet}$ is the number of droplets excreted per cough, L is the viral load in the
 326 respiratory tract in $copies/mL$. According to [34], the viral load of SARS-CoV-2 for children
 327 aging 0-22 is $6.2 \log_{10}$ RNA copies/ml, which is adopted in this study as the occupants are
 328 primarily children in school buildings. Due to the lack of data, other parameters are
 329 estimated using parameters of MERS-CoV in [33]. $V_{droplet}$ is calculated considering the
 330 largest diameter for infectious droplets that best fits the scenario of fomite transmission. The
 331 diameter is set as $100 \mu m$. F_{cough} is set as 12 times per hour. $N_{droplet}$ is set to be 2000 per
 332 cough. Based on the calculation above, α is set to be $1.99E4$. Besides, as the accurate
 333 shedding rate is still not well understood, it is assumed within the range of $(1.8E3, 2.39E4)$,
 334 where the lower bound is set according to [28], and the higher bound is set as 1.2 times of
 335 the estimated value to allow potential higher shedding rate value.
 336

337 5) Dose response of pathogens on mucosa (π). The infectivity is determined based on study
 338 [31]. [31] found that the exponential model $p = 1 - \exp(-d/k)$ can well demonstrate the
 339 dose-response function of SARS-CoV-2, where the constant k ranges from $6.19E4$ to
 340 $7.28E5$. In the paper, k is set as $1.52E5$, representing 50% of contribution from airborne
 341 particles to the total dose. π is set as the inverse of k , which is $6.58E6$.
 342

343 2.1.3. *Risk Assessment*

344 In epidemic dynamics, the basic reproductive number (R_0) is an estimation of a pathogen's
 345 transmission ability of an infectious disease. R_0 is the expected number of cases generated by
 346 one single infected person, supposing all other individuals are susceptible to the epidemic [35].
 347 In this study, R_0 is used to represent the outbreak potential of each pathogen across different
 348 rooms in the building. Given the fomite-mediated transmission model described in the previous
 349 section, R_0 is computed using the next generation matrix method [36], which consists of two
 350 matrices, i.e., the matrix of disease transmission and matrix of host state transition. R_0 is
 351 identified as the dominant eigenvalue of the product of the two matrices, computed using Eq. 5
 352 proposed in [24].
 353

$$\left\{
 \begin{aligned}
 R_0 &= R_{0,F} + R_{0,H} \\
 R_{0,F} &= \frac{a_F}{\gamma} P_{inoculation} P_{pickup} P'(0) \\
 R_{0,H} &= \frac{a_H}{\gamma} P_{inoculation} P_{pickup} P_{deposit} P'(0) \\
 P_{inoculation} &= \frac{\rho \chi}{\mu_H + \rho_{HF} + \rho \chi + \theta_H} \\
 P_{pickup} &= \frac{\frac{N \rho_{FH}}{N \rho_{FH} + \mu_F + \theta_F}}{1 - \frac{\rho_{HF}}{(N \rho_{FH} + \mu_F + \theta_F)(\mu_H + \rho_{HF} + \rho \chi + \theta_H)}} \\
 P_{deposit} &= \frac{\rho_{HF}}{\mu_H + \rho_{HF} + \rho \chi + \theta_H}
 \end{aligned}
 \right. \quad (5)$$

355 $R_{0,F}$ represents direct fomite contamination route, $R_{0,H}$ is hand-fomite contamination route,
 356 $P_{inoculation}$ is the proportion of pathogens that are self-inoculated to susceptible hosts; P_{pickup} is
 357 the proportion of pathogens picked up by hands from fomites; $P_{deposit}$ is the proportion of
 358 pathogens excreted to hands that are deposited to the fomites. $P'(0)$ is the slope of the dose
 359 function, indicating the infectivity of a dose of the pathogen.
 360

361 In the above equations, $a_F = \alpha(1 - \varphi_H)\lambda$, representing the rate pathogens excreted to surfaces,
 362 where α is the shedding rate, φ_H is the proportion that pathogens are shed on hands, both
 363

364 defined in Table 1. λ is the proportion of accessible surfaces, calculated by parameters
365 extracted from the BIM model. $a_H = \alpha\varphi_H$, representing the rate pathogens excreted to hands.
366 Infectious period $1/\gamma$, inoculation rate ρ , and pathogen inactivation rate in hands μ_H and in
367 fomites μ_F , are all pathogen-specific parameters that are defined in Table 1. χ is the proportion
368 of pathogens self-inoculated by susceptible hosts, set as 1 in this study. $\rho_{HF} = \rho_T\tau_{HF}$, indicating
369 the rate of pathogen deposited from hand to fomite, where ρ_T is the rate of fomite touching
370 extracted from the BIM model, τ_{HF} is the transmission efficiency defined in Table 1. θ_H is the
371 effective hand cleaning rate, which is set as the rate of hand washing. N is the occupancy of
372 each room, extracted from the BIM model. $\rho_{FH} = N\rho_T\tau_{FH}\kappa$, representing the rate of pathogen
373 picked up by hands, where τ_{FH} is the transmission efficiency from fomites to hands, κ is the
374 fingertip to surface ratio, set as $\frac{6E-06}{\lambda}$ according to study [24]. θ_F is the effective fomite cleaning
375 rate, which is set as the rate of building cleaning and can be extracted from BIM model.
376

377 In epidemiology literature, R_0 is one of the most widely used indicators of transmission intensity
378 to demonstrate the outbreak potential of an infectious disease in a population. Commonly, $R_0 >$
379 1 means the epidemic begins to spread in the population, $R_0 < 1$ means the disease will
380 gradually disappear, and $R_0 = 1$ means the disease will stay alive and reach a balance in the
381 population. With the increase of R_0 , the outbreak risk will increase, and more severe control
382 measures and policies will be needed [37]. In this study, we categorize the level of outbreak risk
383 into low, mild, moderate, and severe based on the range of R_0 . Specifically, the risk is low when
384 $R_0 < 1$; the risk is mild when $1 \leq R_0 < 1.5$ because there is a fair chance that the transmission
385 will fade out as R_0 is not much larger than 1 [38]; the risk is moderate when $1.5 \leq R_0 < 2$,
386 indicating an epidemic can occur and is likely to do so [39,40]; and the risk is severe when $R_0 >$
387 2 and immediate actions should be taken by facility managers, such as cleaning the surfaces, to
388 reduce the risk.
389

390 **2.2. Web-Based Information Communication System**

391 To better communicate the infection risk to occupants and facility managers, a web-based
392 system was developed to visualize the outbreak risk of different pathogens in each room within
393 a building. Fig. 5 illustrates the architecture of the web-based system, which consists of four
394 modules, i.e., data management, model derivative, web application, and user. The data
395 management module is maintained by the management team and allows them to upload
396 building models. In the model derivative module, the uploaded model is translated into the SVF
397 format which is the format used by the web application. The web application module displays
398 the building model and provides customized functionalities to facilitate visualization of pathogen
399 risk within the building. Finally, the user can access the web-based system and visualize the
400 room-level risk of pathogens. The web-based system is developed using Autodesk Forge that is
401 a collection of APIs to develop cloud-based platforms to access, manage, and visualize design
402 and engineering data. Each module is detailed below.
403

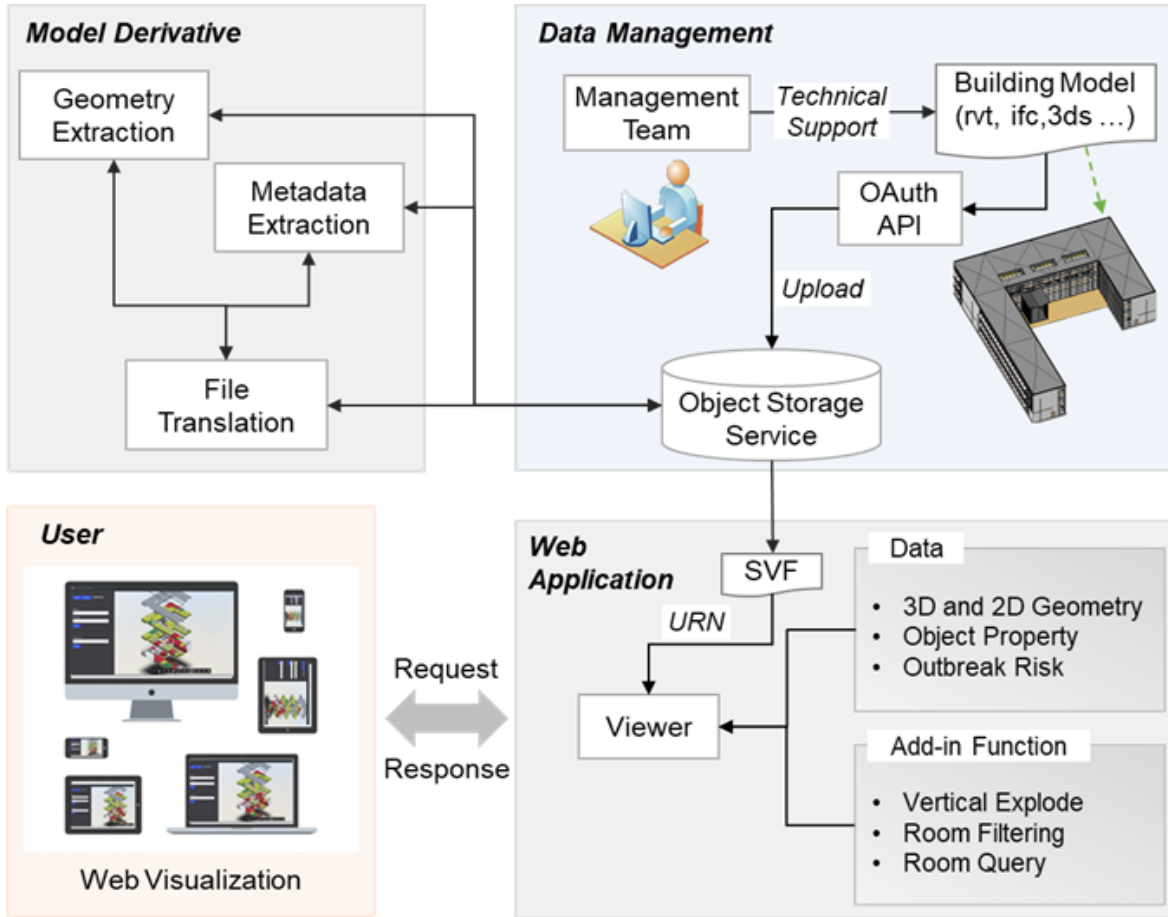


Fig. 5. Web-based alert system

404
405
406

407 The data management module supports a variety of 3D model formats such as rvt, ifc, and 3ds,
408 where rvt is the file format used by the Autodesk Revit; ifc is an open international standard data
409 schema for BIM data that are supported by various software products such as AutoCAD, Revit,
410 and Tekla Structures; 3ds is the file format used by the Autodesk 3ds Max 3D modeling,
411 animation and rendering software. The management team needs to log into their account to
412 obtain authorization from the Forge OAuth API to access the Object Storage Service (OSS).
413 Model files are uploaded to the OSS and stored as objects in buckets. In the second module,
414 the model derivative translates the uploaded model into SVF format and extracts design
415 metadata such as geometric data and object properties (e.g. room area and occupancy). The
416 translated model and extracted data are also stored in the OSS. The model derivative
417 component generates a unique identifier called URN for each translated model. The URN is
418 then fed into the web application for the building model visualization.
419

420 The web application is built on the Forge Viewer API with customized functions. The Viewer API
421 is a WebGL-based JavaScript library to render both 2D and 3D models. It is developed to
422 display translated models generated by the model derivative component. ExpressJS was
423 selected to develop the web application due to its flexibility and scalability. ExpressJS is a
424 prebuilt NodeJS framework that is designed to create server-side web applications [41], and it
425 allows the web application to handle multiple requests concurrently. As such, pathogen risk
426 information can be quickly communicated to facility users even at times of peak traffic of the
427 website. ExpressJS allows the developer to design customized functionalities in the web
428 application. The routing technique was adopted to handle the Hypertext Transfer Protocol

429 (HTTP) request. The routing technique manages the way the web application responds to user
430 requests. This technique is derived from the HTTP method [42] and attached to the ExpressJS
431 router instance. POST and GET methods were used to send and retrieve data from the
432 webserver.

433
434 Three add-in functions were developed to help users visualize the interior layout of the building
435 and color-coded rooms with their corresponding risk levels, as well as search specific room-
436 related disease outbreak risk information. The first add-in function is “vertical explode”, which is
437 used to view each level of the building. This function can help the user visualize the interior and
438 room layout. The facility users can also use this function to visualize the outbreak risk of rooms
439 on each floor and take appropriate practices. For facility managers, the “vertical explode”
440 function enables them to obtain a holistic view of risk distribution at each level and take
441 informed actions, such as limiting the number of occupants and implementing cleaning and
442 disinfection protocols, to control the spread of the disease. This function is integrated with the
443 web-based system, and clicking buttons were created to activate and deactivate it. The second
444 function is “room filtering”, which is used to highlight rooms at different risk levels for a specific
445 pathogen. The user needs to first select one of the three pathogens from the dropdown menu:
446 SARS-CoV-2, Influenza, and norovirus. Thereafter, the user can set a risk threshold to highlight
447 rooms with R_0 greater than a specific value. In addition, different highlighting colors are used to
448 represent different infection risk levels. Low, mild, moderate, and severe risks are represented
449 by color green, blue, celery, and red, respectively. The third function is “room query”, which
450 enables the user to search for a specific room and retrieve infection risk for the three pathogens.
451 The “room query” function is displayed as a search box on the web-based system. The users
452 can easily find the potential risk of a specific room using this function. Finally, end users can
453 access the web-based information communication system and obtain information about
454 outbreak risk in each room of the building through various channels, including laptops,
455 smartphones, and tablets.

456
457 **3. Case Study**

458 A hypothetical case study is used as an example to demonstrate the efficacy of the proposed
459 framework and the newly developed web-based system. The building information model of a
460 six-floor school building with 221,000 square feet is used. The building contains classrooms and
461 faculty and graduate assistant offices.

462
463 **3.1. Disease Outbreak Risk in Different Rooms**

464 The room types considered in the case study include offices and classrooms. Five offices and
465 five classrooms were selected. The venue-specific parameters of the rooms are extracted and
466 listed in Table 3, and the computed R_0 values of the three diseases are listed in Table 4.

467
468 **Table 3.** Venue-specific parameters in representative rooms

Room Type	Room #	Accessible surface area (square feet)	Proportion of accessible surface	Occupancy (number of people)	Rate of fomite touching (times per hour)
Classroom	#1	45.5	0.018	36	45 (30, 60)
	#2	45.5	0.017	37	45 (30, 60)
	#3	176.3	0.138	19	45 (30, 60)
	#4	1328.9	0.194	91	45 (30, 60)
	#5	410.9	0.151	26	45 (30, 60)
Office	#1	36.6	0.052	2	12 (0, 30)

#2	106.8	0.115	13	12 (0, 30)
#3	52.1	0.062	10	12 (0, 30)
#4	1289.8	0.306	9	12 (0, 30)
#5	53.7	0.053	15	12 (0, 30)

469

470

Table 4. R_0 values of the three diseases of representative rooms

Room Type	Room #	R_0 values		
		Influenza	Norovirus	COVID-19
Classroom	#1	0.078	9.704 ²	0.962
	#2	0.079	10.441 ²	0.970
	#3	0.014	0.092	0.168
	#4	0.237	2.603 ²	1.803 ¹
	#5	0.020	0.117	0.224
Office	#1	0.002	0.023	0.022
	#2	0.010	0.073	0.118
	#3	0.008	0.098	0.099
	#4	0.007	0.023	0.078
	#5	0.011	0.169	0.146

471 Note: The superscripts indicate the risk level of the diseases, where 1 represents a moderate
472 risk level and 2 represents a severe risk level. Values without superscripts indicate the risk level
473 is low.

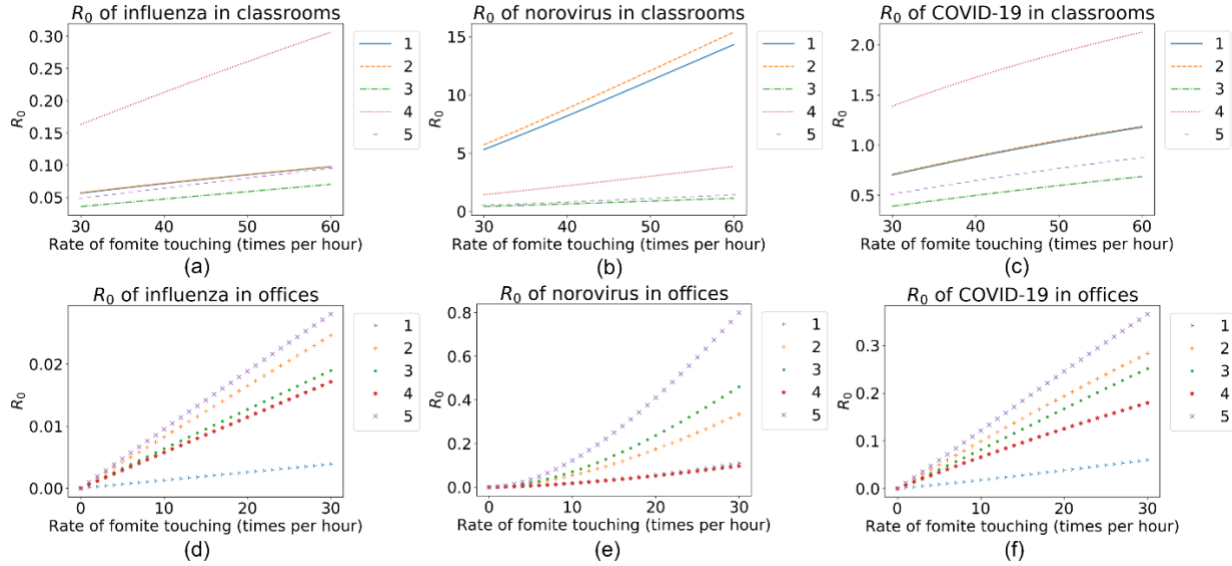
474

475 From Table 4, the values of R_0 vary across different rooms and different diseases. R_0 values in
476 offices are smaller than the values in classrooms, which stems from the small occupancy and
477 the low rate of fomite touching in offices compared to those in classrooms. For influenza, the R_0
478 values in all the rooms are less than 1, indicating that influenza is unlikely to outbreak in the
479 building through the fomite-mediated transmission. This could be partially explained by the
480 relatively short infectious period, high inactivation rate in hands, low hand-to-fomite pathogen
481 transmission efficiency, and relatively low infectiousness with the same amount of pathogens.
482 For COVID-19, the R_0 values in all rooms are higher than those of influenza, and the risk in
483 Classroom 4 reaches a moderate level, indicating that COVID-19 has the potential to outbreak
484 in the classroom. COVID-19 has a relatively high outbreak risk in most cases because it has a
485 high shedding rate, small surface inactivation rate, and high transfer efficiency from fomites to
486 hands. For norovirus, the R_0 values are high in most classrooms, which might be because of its
487 high infectivity, long infection period, and high hand-to-fomite transmission efficiency compared
488 to the other two diseases. This finding also aligns with the trend obtained in [24]. The above
489 results prove that the outbreak risk of an infectious disease is influenced by both venue-specific
490 and pathogen-specific parameters, which highlights the significance of integrating BIM and the
491 pathogen transmission model in assessing spatial-varying disease outbreak risk.

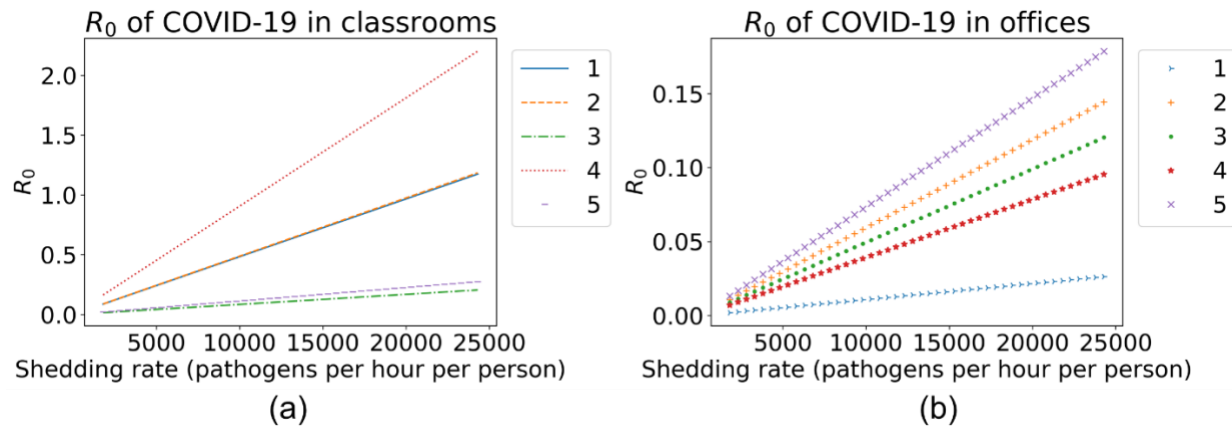
492

493 Sensitivity analysis was further conducted to evaluate the influence of the rate of fomite
494 touching (ρ_T) and the shedding rate (α) of SARS-COV-2 on R_0 based on the estimated ranges
495 of the two parameters (listed in Table 2). Fig. 6 illustrates the changes in R_0 with the increase of
496 ρ_T for all three diseases in both classrooms and offices. From Fig. 6, the disease outbreak risk
497 increases as the increase of ρ_T . The values of R_0 for norovirus and COVID-19 in Classroom 1,
498 2, and 4 may exceed 1 with the increase of ρ_T . On the other hand, the infection risk in offices

499 and that for influenza in classrooms will remain low even occupants touch objects in the rooms
500 more frequently. Therefore, it is particularly important to educate students in classrooms with
501 relatively high occupancy to not touch the common areas frequently. Fig. 7 illustrates the
502 changes in R_0 of COVID-19 with varying shedding rates. From the figure, α has a significant
503 impact on the outbreak risk of COVID-19 in Classroom 1, 2, and 4. Therefore, for classrooms
504 with relatively large occupancy, control strategies should be taken to reduce pathogen shedding
505 from the occupants, such as using face masks, and covering the mouth when coughing.
506



507
508
509
Fig. 6. R_0 values with various rates of fomite touching (ρ_T)



510
511
512
513
Fig. 7. R_0 of COIVD-19 with various shedding rate (α)

3.2. Influence of Cleaning Practice

514 Cleaning is an effective strategy to reduce fomite-mediated pathogen transmission in built
515 environments [43]. This study examined the impact of surface cleaning at different times per day
516 on reducing the disease outbreak risk. The timing of each cleaning practice is not included in
517 the disease transmission model and the average R_0 is estimated on an hourly basis. Fig. 8
518 illustrates the changes in R_0 with respect to various times of surface cleaning each day.
519

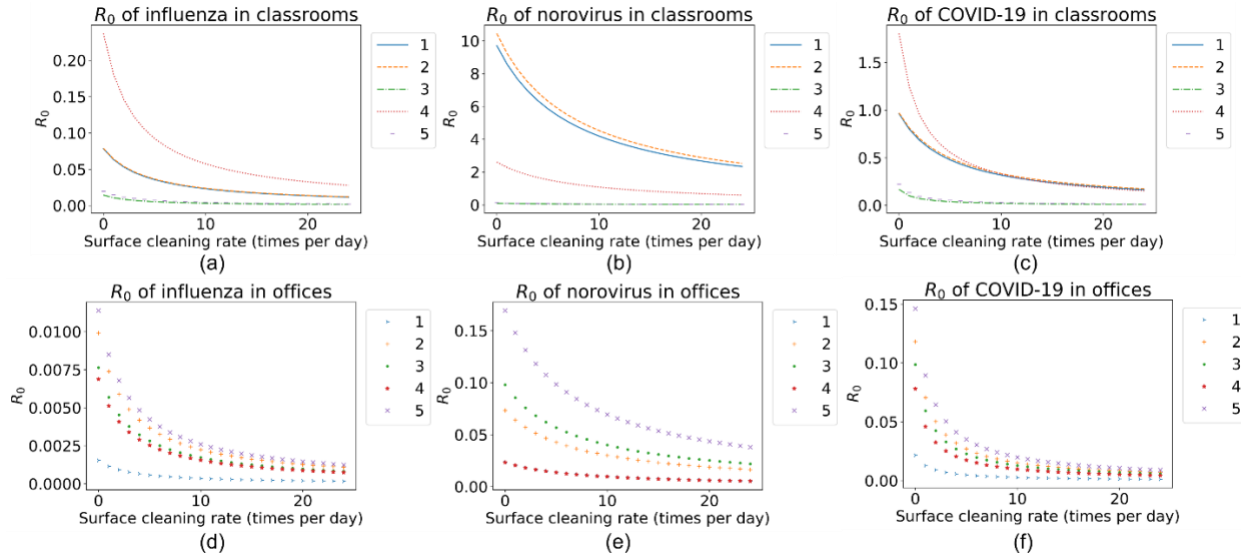


Fig. 8. R_0 values with various times of surface cleaning per day

From Fig. 8, surface cleaning can significantly reduce the outbreak risk of all three diseases in both classrooms and offices. Based on the analysis, different surface cleaning practices can be applied to different rooms to reduce the risks to an acceptable low level. Cleaning the surface five times per day will decrease R_0 by over 50%, compared to no surface cleaning. Considering the ongoing outbreak of COVID-19, classrooms with high occupancy (e.g., Classroom 4) should be given particular attention on surface cleaning. Cleaning surfaces at least two times per day is needed to achieve a low risk level. For norovirus, classrooms with relatively large occupancy (e.g., Classroom 1, 2, and 4) will require more frequent surface cleaning to reduce the outbreak risk to the low level. Other complementary strategies, such as increasing hand washing and limiting occupancy, should be adopted to maintain a low level of outbreak risks.

3.3. Infection risk visualization via web-based system

Fig. 9 presents the user interface of the developed web-based system. The developed web application provides an intuitive and responsive user interface to visualize outbreak risk information in the building. The facility manager and user can navigate to the interior model to visualize the interior layout of the building using the “Interior Model” button. The user can select and visualize risk-related information for different diseases: COVID-19, influenza, and norovirus. Fig. 10 illustrates the developed web visualization tool.

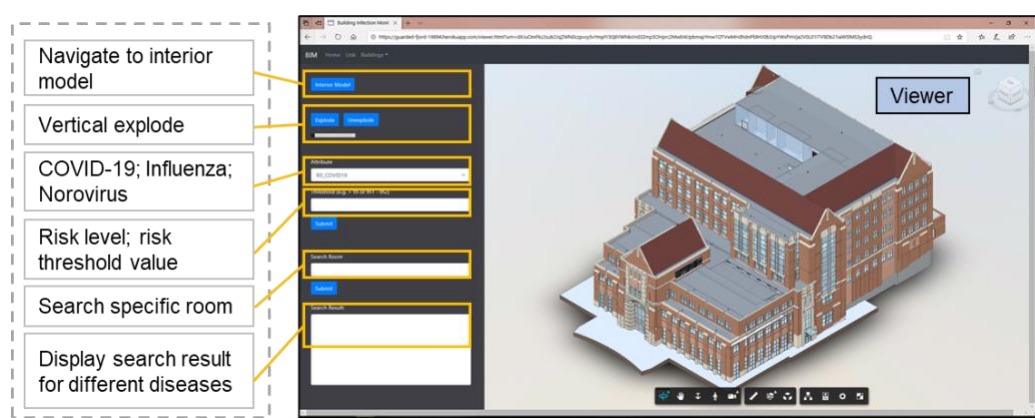
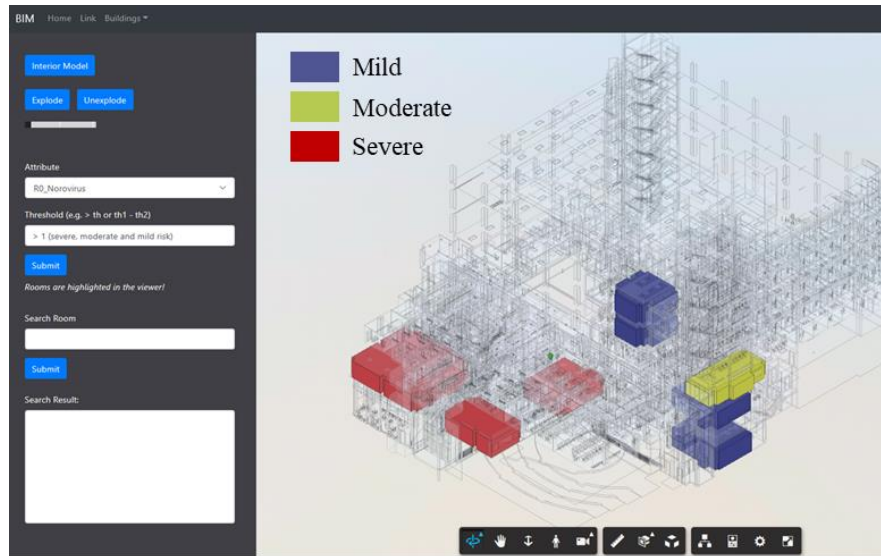
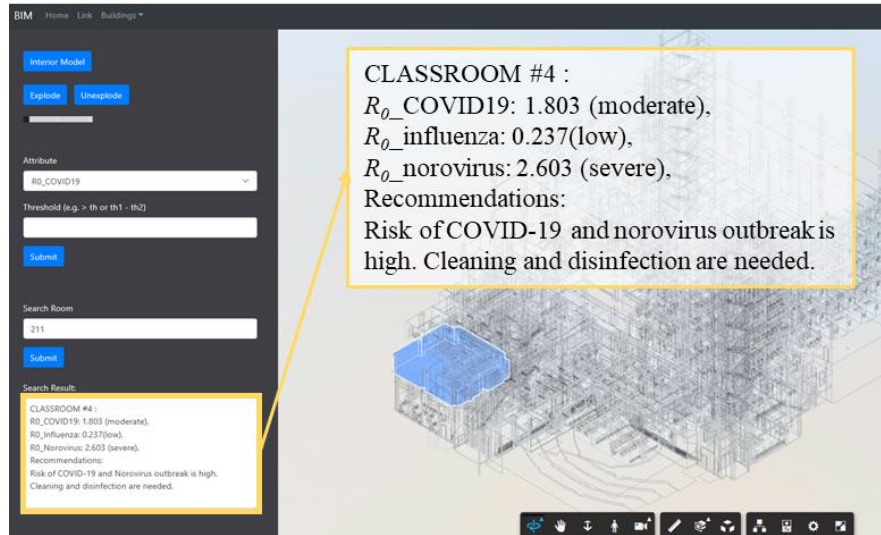


Fig. 9. The user interface of the developed web-based alert system



(a)



(b)

Fig. 10. Demonstration of pathogen risk visualization. (a) room filtering based on risk value threshold; (b) search specific room

As shown in Fig. 10, room filtering and room query functions can help the user easily locate rooms with high risk and query risk information for a specific room. Specifically, Fig. 10 (a) shows an exemplary output of the room filtering function that highlights the rooms with R_0 value greater than 1 for COVID-19. Fig. 10 (b) displays an example of the room query function in the web system. The pathogen risk information for influenza, norovirus, and COVID-19 is retrieved with corresponding recommendations. With the web-based information communication system, facility managers can take important measures to control the spread of diseases, such as designing appropriate cleaning and disinfection strategies, promoting hand hygiene, reducing maximum occupancy, and accommodating facility usage schedule based on risk distribution across rooms within the building. For instance, deep cleaning and disinfection are required for rooms with severe outbreak risk. In addition, facility managers can post signs at these high-risk areas to

560 remind occupants to take essential practices such as social distancing and hand hygiene. The
561 web-based system will also keep facility users, including teachers, students, and other staff,
562 aware of up-to-date outbreak risk information within the building, and thus taking informed actions
563 to avoid further spread of diseases. For example, facility users can avoid entering rooms with high
564 outbreak risk.

565

566 **4. Discussion**

567 The results and insights derived from the analysis have important implications on adaptive built
568 environment management to prevent infectious disease outbreak and respond to on-going
569 pandemic. Due to varying building characteristics, occupancy levels, and pathogen parameters,
570 the microbial burdens and outbreak risks differ significantly even in the same building,
571 highlighting the need for spatially-adaptive management of the built environment. The proposed
572 method automates the batch process for simulation and prediction of outbreak risks for different
573 pathogens at the room level, and visualizes the risks for adaptive management. The results on
574 outbreak risks at room level enables the paradigm for spatially-adaptive management of the
575 built environment. With the new streams of risk information, customizable interventions can be
576 designed. For instance, in consistent with the practice during the COVID-19 pandemic, reducing
577 the accessible surfaces in rooms and restricting the occupancy in the room are some of the
578 effective strategies to reduce the outbreak risks. The spatially-varying risk information can also
579 guide the facility managers to pay close attention to high-risk areas by adopting more frequent
580 disinfection practices.

581

582 A BIM-based information system is developed to extract the necessary information for modeling
583 infection within buildings, and to visualize the derived information in an easy-to-understand and
584 convenient way through web pages. As such, the information-driven interventions could
585 alleviate the pathogenic burdens in the buildings to prevent the spread of infectious diseases.
586 Providing information to end-users is critically important for them to change behaviors. Human
587 behavior plays an important role in the transmission of pathogens such as the SARS-Cov-2.
588 Changing behaviors is critical to preventing transmission. Providing timely and contextual
589 information can be a promising option to motive the change of human behaviors. With the room-
590 level outbreak risk information, the users could be motivated or persuaded by the visualized
591 risks to practice appropriate behaviors such as wearing a mask, social distancing, and hand-
592 washing. The facility managers can use the information to conduct knowledge-based
593 management, such as limiting the occupancy in the room, managing crowd traffic, and
594 rearranging room layout.

595

596 This study has some limitations that deserve future research. First, the model does not consider
597 factors such as sunlight exposure, humidity, and airflow that may impact the persistence and
598 transmission of pathogens in built environments. This is mainly because the quantitative
599 impacts of these factors on pathogen persistence and transmission are largely ambiguous, if not
600 unknown. If these impacts can be quantified and the environmental parameters can be
601 monitored and modeled in BIM, our proposed framework can be extended to incorporate these
602 factors. Second, the computation of R_0 only considers the fomite-mediated transmission, and
603 does not consider the airborne and close contact transmission. Microbial pathogens may have
604 different transmission routes, including airborne, close-contact, and fomite-based transmission.
605 This study focused on fomite-based transmission to illustrate the modeling approach for
606 assessing the outbreak risks, and demonstrate the efficacy of the developed information system
607 to guide infection control practices and building operations. To fully assess the exposure risks
608 and outbreak potentials, all important routes need to be considered. In addition, the outbreak
609 potentials of a variety of pathogens can be considered together to develop an aggregate index,

610 which could be more intuitive for occupants and facility managers who are not public health
611 experts. Third, the system mainly relies on static models and does not make full use of dynamic
612 and real-time data regarding built environments and occupant behaviors such as presence and
613 interactions with objects. In future studies, the internet of things sensors can be installed in the
614 buildings and algorithms can be developed to retrieve dynamic data for integration with the
615 models for accurate and robust risk estimation. Fourth, the web-based system can be further
616 improved by connecting it with smart devices such as robots for automated cleaning and
617 disinfection and smartphones for precision notifications.

618 619 **5. Conclusions**

620 This study creates and tests a computational framework and tools to explore the connections
621 among built environment, occupant behavior, and pathogen transmission. Using BIM-based
622 simulations, building-occupant characteristics, such as occupancy and accessible surface, are
623 extracted as venue-specific parameters. The fomite-mediated transmission model is used to
624 predict the contamination risks in the built environment by calculating a room-by-room basic
625 reproductive number R_0 , based on which the level of infection risk at each room is characterized
626 into low, mild, moderate, and severe. A web-based system is then created to communicate the
627 infection risk and outbreak potential information within buildings to occupants and facility
628 managers. The case study demonstrated the efficacy of the proposed methods and developed
629 systems. Practically, the method and system can be used in a variety of built environments,
630 especially, schools, hospitals, and airports, where transmission of infectious pathogens is of
631 particular concern. The outbreak risks predicted at room resolutions can inform the facility
632 managers to determine room disinfection and cleaning frequency, schedule, and standard. In
633 addition, appropriate operational interventions including access control, occupancy limits, social
634 distancing, and room arrangement (e.g. reducing the number of tables and chairs) can be
635 designed based on the derived information. The occupants can access the useful information
636 via webpage to plan their visit and staying time in the facilities, and practice appropriate
637 personal hygiene and cleaning practice based on the information. – Shuai Li

638 639 **Acknowledgement**

640 This research was funded by the U.S. National Science Foundation (NSF) via Grant 2026719,
641 1952140, and 2038967. The authors gratefully acknowledge NSF's support. Any opinions,
642 findings, recommendations, and conclusions in this paper are those of the authors, and do not
643 necessarily reflect the views of NSF, the University of Tennessee, Knoxville, and the University
644 of Texas at San Antonio. The authors also acknowledge Zhouyang Li's assistance in developing
645 the web-based system.

646 647 **Reference**

- 648 [1] B. Stephens, P. Azimi, M.S. Thoennes, M. Heidarnejad, J.G. Allen, J.A. Gilbert,
649 Microbial Exchange via Fomites and Implications for Human Health, *Curr. Pollut. Reports.*
650 5 (2019) 198–213. <https://doi.org/10.1007/s40726-019-00123-6>.
- 651 [2] ScienceDaily, How quickly viruses can contaminate buildings -- from just a single
652 doorknob, (2014). <https://www.sciencedaily.com/releases/2014/09/140908093640.htm>
653 (accessed August 7, 2020).
- 654 [3] S.A. Boone, C.P. Gerba, The occurrence of influenza A virus on household and day care
655 center fomites, *J. Infect.* 51 (2005) 103–109. <https://doi.org/10.1016/j.jinf.2004.09.011>.
- 656 [4] E. Dong, H. Du, L. Gardner, An interactive web-based dashboard to track COVID-19 in
657 real time, *Lancet Infect. Dis.* 20 (2020) 533–534. [https://doi.org/10.1016/S1473-3099\(20\)30120-1](https://doi.org/10.1016/S1473-3099(20)30120-1).
- 658 [5] B. Pastorino, F. Touret, M. Gilles, X. de Lamballerie, R.N. Charrel, Prolonged Infectivity of

660 SARS-CoV-2 in Fomites, *Emerg. Infect. Dis.* 26 (2020).
661 <https://doi.org/10.3201/eid2609.201788>.

662 [6] E. Goldman, Exaggerated risk of transmission of COVID-19 by fomites, *Lancet Infect. Dis.* 20 (2020) 892–893. [https://doi.org/10.1016/S1473-3099\(20\)30561-2](https://doi.org/10.1016/S1473-3099(20)30561-2).

663 [7] E.L. Jones, A. Kramer, M. Gaither, C.P. Gerba, Role of fomite contamination during an outbreak of norovirus on houseboats, *Int. J. Environ. Health Res.* 17 (2007) 123–131. <https://doi.org/10.1080/09603120701219394>.

664 [8] R.L. Fankhauser, S.S. Monroe, J.S. Noel, C.D. Humphrey, J.S. Bresee, U.D. Parashar, T. Ando, R.I. Glass, Epidemiologic and molecular trends of “Norwalk-like viruses” associated with outbreaks of gastroenteritis in the United States, *J. Infect. Dis.* 186 (2002) 1–7.

665 [9] J.A. Gilbert, B. Stephens, Microbiology of the built environment, *Nat. Rev. Microbiol.* 16 (2018) 661–670. <https://doi.org/10.1038/s41579-018-0065-5>.

666 [10] J. Zhao, J.E. Eisenberg, I.H. Spicknall, S. Li, J.S. Koopman, Model Analysis of Fomite Mediated Influenza Transmission, *PLoS One.* 7 (2012) e51984. <https://doi.org/10.1371/journal.pone.0051984>.

667 [11] I.H. Spicknall, J.S. Koopman, M. Nicas, J.M. Pujol, S. Li, J.N.S. Eisenberg, Informing Optimal Environmental Influenza Interventions: How the Host, Agent, and Environment Alter Dominant Routes of Transmission, *PLoS Comput. Biol.* 6 (2010) e1000969. <https://doi.org/10.1371/journal.pcbi.1000969>.

668 [12] S. Li, J.N.S. Eisenberg, I.H. Spicknall, J.S. Koopman, Dynamics and control of infections transmitted from person to person through the environment, *Am. J. Epidemiol.* 170 (2009) 257–265.

669 [13] M. King, M. López-García, K.P. Atedoghu, N. Zhang, A.M. Wilson, M. Weterings, W. Hiwar, S.J. Dancer, C.J. Noakes, L.A. Fletcher, Bacterial transfer to fingertips during sequential surface contacts with and without gloves, *Indoor Air.* (2020) ina.12682. <https://doi.org/10.1111/ina.12682>.

670 [14] A.M. Wilson, M.-F. King, M. López-García, M.H. Weir, J.D. Sexton, R.A. Canales, G.E. Kostov, T.R. Julian, C.J. Noakes, K.A. Reynolds, Evaluating a transfer gradient assumption in a fomite-mediated microbial transmission model using an experimental and Bayesian approach, *J. R. Soc. Interface.* 17 (2020) 20200121. <https://doi.org/10.1098/rsif.2020.0121>.

671 [15] P. Zhao, P.T. Chan, Y. Gao, H.W. Lai, T. Zhang, Y. Li, Physical factors that affect microbial transfer during surface touch, *Build. Environ.* 158 (2019) 28–38. <https://doi.org/10.1016/j.buildenv.2019.05.005>.

672 [16] S.W. Kembel, J.F. Meadow, T.K. O'Connor, G. Mhuireach, D. Northcutt, J. Kline, M. Moriyama, G.Z. Brown, B.J.M.M. Bohannan, J.L. Green, T.K. O'Connor, G. Mhuireach, D. Northcutt, J. Kline, M. Moriyama, G.Z. Brown, B.J.M.M. Bohannan, J.L. Green, Architectural design drives the biogeography of indoor bacterial communities, *PLoS One.* 9 (2014) e87093. <https://doi.org/10.1371/journal.pone.0087093>.

673 [17] S.W. Kembel, E. Jones, J. Kline, D. Northcutt, J. Stenson, A.M. Womack, B.J.M. Bohannan, G.Z. Brown, J.L. Green, Architectural design influences the diversity and structure of the built environment microbiome, *ISME J.* 6 (2012) 1469–1479. <https://doi.org/10.1038/ismej.2011.211>.

674 [18] R.I. Adams, M. Miletto, J.W. Taylor, T.D. Bruns, The diversity and distribution of fungi on residential surfaces, *PLoS One.* 8 (2013). <https://doi.org/10.1371/journal.pone.0078866>.

675 [19] R.I. Adams, A.C. Bateman, H.M. Bik, J.F. Meadow, Microbiota of the indoor environment: a meta-analysis, *Microbiome.* 3 (2015) 49. <https://doi.org/10.1186/s40168-015-0108-3>.

676 [20] J.F. Meadow, A.E. Alricher, S.W. Kembel, M. Moriyama, T.K. O'Connor, A.M. Womack, G.Z. Brown, J.L. Green, B.J.M. Bohannan, Bacterial communities on classroom surfaces vary with human contact, *Microbiome.* 2 (2014). <https://doi.org/10.1186/2049-2618-2-7>.

711 [21] B. Stephens, What Have We Learned about the Microbiomes of Indoor Environments?,
 712 MSystems. 1 (2016). <https://doi.org/10.1128/msystems.00083-16>.

713 [22] C. Eastman, P. Teicholz, R. Sacks, K. Liston, BIM handbook: A guide to building
 714 information modeling for owners, managers, designers, engineers and contractors, John
 715 Wiley & Sons, 2011.

716 [23] X. Wang, P.E.D. Love, M.J. Kim, C.S. Park, C.P. Sing, L. Hou, A conceptual framework
 717 for integrating building information modeling with augmented reality, Autom. Constr. 34
 718 (2013) 37–44. <https://doi.org/10.1016/j.autcon.2012.10.012>.

719 [24] A.N.M. Kraay, M.A.L. Hayashi, N. Hernandez-Ceron, I.H. Spicknall, M.C. Eisenberg, R.
 720 Meza, J.N.S. Eisenberg, Fomite-mediated transmission as a sufficient pathway: A
 721 comparative analysis across three viral pathogens 11 Medical and Health Sciences 1117
 722 Public Health and Health Services, BMC Infect. Dis. 18 (2018) 1–13.
 723 <https://doi.org/10.1186/s12879-018-3425-x>.

724 [25] R. Volk, J. Stengel, F. Schultmann, Building Information Modeling (BIM) for existing
 725 buildings - Literature review and future needs, Autom. Constr. 38 (2014) 109–127.
 726 <https://doi.org/10.1016/j.autcon.2013.10.023>.

727 [26] R. Alshorafa, E. Ergen, Determining the level of development for BIM implementation in
 728 large-scale projects: A multi-case study, Eng. Constr. Archit. Manag. (2019).
 729 <https://doi.org/10.1108/ECAM-08-2018-0352>.

730 [27] N. Zhang, Y. Li, Transmission of Influenza A in a Student Office Based on Realistic
 731 Person-to-Person Contact and Surface Touch Behaviour, Int. J. Environ. Res. Public
 732 Health. 15 (2018) 1699. <https://doi.org/10.3390/ijerph15081699>.

733 [28] A.N.M. Kraay, M.A.L. Hayashi, D.M. Berendes, J.S. Sobolik, J.S. Leon, B.A. Lopman, (A
 734 Kraay, J. Sobolik, J. Leon, Risk of fomite-mediated transmission of SARS-CoV-2 in child
 735 daycares, schools, and offices: a modeling study, MedRxiv. (2020)
 736 2020.08.10.20171629. <https://doi.org/10.1101/2020.08.10.20171629>.

737 [29] Visual scripting environment for designers - Dynamo, (n.d.). <https://dynamobim.org/>
 738 (accessed August 7, 2020).

739 [30] J. Bullard, K. Dust, D. Funk, J.E. Strong, D. Alexander, L. Garnett, C. Boodman, A. Bello,
 740 A. Hedley, Z. Schiffman, K. Doan, N. Bastien, Y. Li, P.G. Van Caeseele, G. Poliquin,
 741 Predicting infectious SARS-CoV-2 from diagnostic samples, Clin. Infect. Dis. (2020).
 742 <https://doi.org/10.1093/cid/ciaa638>.

743 [31] X. Zhang, J. Wang, Deducing the Dose-response Relation for Coronaviruses from
 744 COVID-19, SARS and MERS Meta-analysis Results, MedRxiv. (2020)
 745 2020.06.26.20140624. <https://doi.org/10.1101/2020.06.26.20140624>.

746 [32] Homeland Security, Estimated Surface Decay of SARS-CoV-2 (virus that causes COVID-
 747 19), (n.d.). <https://www.dhs.gov/science-and-technology/sars-calculator> (accessed
 748 August 7, 2020).

749 [33] S. Xiao, Y. Li, M. Sung, J. Wei, Z. Yang, A study of the probable transmission routes of
 750 MERS-CoV during the first hospital outbreak in the Republic of Korea, Indoor Air. 28
 751 (2018) 51–63. <https://doi.org/10.1111/ina.12430>.

752 [34] L.M. Yonker, A.M. Neilan, Y. Bartsch, A.B. Patel, J. Regan, P. Arya, E. Gootkind, G.
 753 Park, M. Hardcastle, A. St. John, L. Appleman, M.L. Chiu, A. Fialkowski, D. De la Flor, R.
 754 Lima, E.A. Bordt, L.J. Yockey, P. D'Avino, S. Fischinger, J.E. Shui, P.H. Lerou, J. V.
 755 Bonventre, X.G. Yu, E.T. Ryan, I. V. Bassett, D. Irimia, A.G. Edlow, G. Alter, J.Z. Li, A.
 756 Fasano, Pediatric SARS-CoV-2: Clinical Presentation, Infectivity, and Immune
 757 Responses, J. Pediatr. (2020). <https://doi.org/10.1016/j.jpeds.2020.08.037>.

758 [35] C. Fraser, C.A. Donnelly, S. Cauchemez, W.P. Hanage, M.D. Van Kerkhove, T.D.
 759 Hollingsworth, J. Griffin, R.F. Baggaley, H.E. Jenkins, E.J. Lyons, T. Jombart, W.R.
 760 Hinsley, N.C. Grassly, F. Balloux, A.C. Ghani, N.M. Ferguson, A. Rambaut, O.G. Pybus,
 761 H. Lopez-Gatell, C.M. Alpuche-Aranda, I.B. Chapela, E.P. Zavala, D. Ma. Espejo

762 Guevara, F. Checchi, E. Garcia, S. Hugonnet, C. Roth, Pandemic potential of a strain of
763 influenza A (H1N1): Early findings, *Science* (80-). 324 (2009) 1557–1561.
764 <https://doi.org/10.1126/science.1176062>.

765 [36] O. Diekmann, J.A.P. Heesterbeek, J.A.J. Metz, On the definition and the computation of
766 the basic reproduction ratio R_0 in models for infectious diseases in heterogeneous
767 populations, *J. Math. Biol.* 28 (1990) 365–382. <https://doi.org/10.1007/BF00178324>.

768 [37] B. Ridenhour, J.M. Kowalik, D.K. Shay, Unraveling R_0 : Considerations for public health
769 applications, *Am. J. Public Health.* 108 (2018) S445–S454.
770 <https://doi.org/10.2105/AJPH.2013.301704>.

771 [38] C.T. Bauch, T. Oraby, Assessing the pandemic potential of MERS-CoV, *Lancet.* 382
772 (2013) 662–664. [https://doi.org/10.1016/S0140-6736\(13\)61504-4](https://doi.org/10.1016/S0140-6736(13)61504-4).

773 [39] D.N. Fisman, G.M. Leung, M. Lipsitch, Nuanced risk assessment for emerging infectious
774 diseases, *Lancet.* 383 (2014) 189–190. [https://doi.org/10.1016/S0140-6736\(13\)62123-6](https://doi.org/10.1016/S0140-6736(13)62123-6).

775 [40] J.R. Koo, A.R. Cook, M. Park, Y. Sun, H. Sun, J.T. Lim, C. Tam, B.L. Dickens,
776 Interventions to mitigate early spread of SARS-CoV-2 in Singapore: a modelling study,
777 *Lancet Infect. Dis.* 20 (2020) 678–688. [https://doi.org/10.1016/S1473-3099\(20\)30162-6](https://doi.org/10.1016/S1473-3099(20)30162-6).

778 [41] M. Satheesh, B.J. D'mello, J. Krol, *Web development with MongoDB and NodeJs*, Packt
779 Publishing Ltd, 2015.

780 [42] R. Fielding, J. Gettys, J. Mogul, H. Frystyk, L. Masinter, P. Leach, T. Berners-Lee,
781 Hypertext transfer protocol—HTTP/1.1, (1999).

782 [43] H. Lei, S. Xiao, B.J. Cowling, Y. Li, Hand hygiene and surface cleaning should be paired
783 for prevention of fomite transmission, *Indoor Air.* 30 (2020) 49–59.
784 <https://doi.org/10.1111/ina.12606>.

785 [44] C. Nicolaides, D. Avraam, L. Cueto-Felgueroso, M.C. González, R. Juanes, Hand-
786 Hygiene Mitigation Strategies Against Global Disease Spreading through the Air
787 Transportation Network, *Risk Anal.* 40 (2020) 723–740.
788 <https://doi.org/10.1111/risa.13438>.

789 [45] R.I. Adams, S. Bhangar, K.C. Dannemiller, J.A. Eisen, N. Fierer, J.A. Gilbert, J.L. Green,
790 L.C. Marr, S.L. Miller, J.A. Siegel, B. Stephens, M.S. Waring, K. Bibby, Ten questions
791 concerning the microbiomes of buildings, *Build. Environ.* 109 (2016) 224–234.
792 <https://doi.org/10.1016/j.buildenv.2016.09.001>.

793 [46] J.A. Gilbert, B. Stephens, Microbiology of the built environment, *Nat. Rev. Microbiol.* 16
794 (2018) 661–670. <https://doi.org/10.1038/s41579-018-0065-5>.

795

796